Transport Aircraft System Identification Using Roll and Yaw Oscillatory Wind Tunnel Data

Patrick C. Murphy*
NASA Langley Research Center, Hampton, VA, 23681-2199

Vladislav Klein†
National Institute of Aerospace, NASA Langley Research Center, Hampton, VA, 23681-2199

Continued studies have been undertaken to investigate and develop aerodynamic models that predict aircraft response in nonlinear unsteady flight regimes for transport configurations. The models retain conventional static and dynamic terms but replace conventional acceleration terms with indicial functions. In the Subsonic Fixed Wing Project of the NASA Fundamental Aeronautics Program and the Integrated Resilient Aircraft Controls project of the NASA Aviation Safety Program one aspect of the research is to apply these current developments to transport configurations to facilitate development of advanced simulation and control design technology. This paper continues development and application of a more general modeling methodology to the NASA Langley Generic Transport Model, a sub-scale flight test vehicle. In the present study models for the lateral-directional aerodynamics are developed.

Nomenclature

A_j, B_j	=	Fourier coefficients
a, b_1	=	deficiency function parameters
b	=	wing span, ft
C_l,C_n,C_Y	=	rolling-moment, yawing-moment, and side-force coefficients
$\bar{c}$	=	mean aerodynamic chord, ft
f	=	frequency, Hz
$F_{a\beta}$	=	deficiency functions
k	=	reduced frequency, $\pi bf/V$
m	=	number of harmonics in Fourier expansion
N	=	number of data points
p, r	=	roll and yaw rates, rad/sec
R^2	=	multiple correlation coefficient or coefficient of determination
s	=	estimated standard error
S	=	reference area, ft^2
T	=	dimensional time constant, sec
t	=	time, sec
V	=	velocity, fps
α	=	angle of attack, rad or deg
α_0	=	mean (nominal) angle of attack, rad or deg
β	=	sideslip angle, rad or deg
ϕ	=	roll angle, rad or deg
η	=	state variable
σ	=	standard error

* Senior Research Engineer, Dynamic Systems & Control Branch, Mail Stop 308, Associate Fellow.
† Professor Emeritus, Dynamic Systems & Control Branch, Mail Stop 308, Associate Fellow.

τ = dummy integration variable

τ_1 = non-dimensional time constant, $\frac{1}{b_1}\left(\frac{2V}{b}\right)$

ω = angular frequency, rad/sec

ψ = yaw angle, rad or deg

subscripts

A = amplitude

a = Y, n, or l

Aerodynamic Derivatives

$$C_{a_\beta} = \frac{\partial C_a}{\partial \beta} \quad \text{where } a = Y, n, \text{ or } l$$

$$C_{a_p} = \frac{b}{2V}\frac{\partial C_a}{\partial p},\ C_{a_r} = \frac{b}{2V}\frac{\partial C_a}{\partial r}$$

I. Introduction

This paper is a continuation of research dealing with identification of a generic transport aircraft from wind tunnel data. A general model formulation of the transport aircraft is considered as a wing-tail configuration with unsteady and nonlinear effects on the wing and tail and their mutual interference. Theoretical background for model postulation can be found in reports by Jones[1], Tobak[2], and Klein[3]. The first results of generic aircraft transport aircraft identification were given by Kharabrov[4]. Presented in Ref. 4 is a state-space mathematical model of longitudinal nonlinear and unsteady aerodynamics from steady and oscillatory wind tunnel data. These data were generated at different angles of attack, frequencies, and amplitudes. The results were presented for a body, body-wing, and body-wing-tail (baseline) configuration, in the form of graphs of aerodynamic coefficients and in-phase and out-of-phase components against nominal angles of attack for different amplitudes and frequencies.

In Ref. 5 the wind tunnel data from Ref. 4 were analyzed using the mathematical model in Ref. 4 and the newly developed model based on indicial functions for the wing, the body-tail and the downwash angle at the tail. The two models differ mainly in the formulation of unsteady aerodynamics. All models with estimated parameters fit the measured data well, however, some unexpected values were obtained due to identification problems associated with the data. These problems were discussed in more detail in Ref. 6.

In order to obtain an extensive and detailed aerodynamic data base, steady and dynamic, low-speed wind tunnel tests were conducted in 2001, 2003, 2007, and 2009, in the NASA Langley 14x22 wind tunnel. Earlier experiments[7,8] conducted in 2001 and 2003 included lateral steady and oscillatory data but these tests were not designed for unsteady model identification. Oscillatory data were only measured at three frequencies which is insufficient for estimation of unsteady aerodynamic terms.

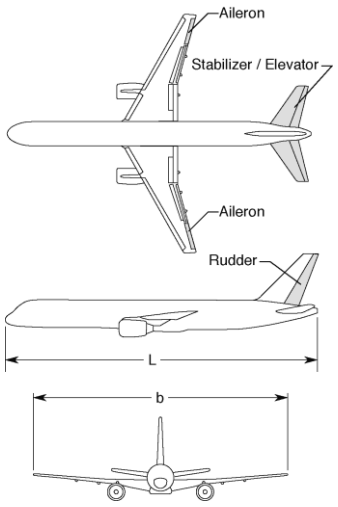

S = 5.90 ft^2, $\bar{c}$ = 0.915 ft, b = 6.85 ft

Figure 1. Model Geometry for NASA experimental sub-scale aircraft.

Experiments in the last two years, included tests specifically designed with a range of frequencies to allow unsteady model identification. Testing in 2007 emphasized the longitudinal dynamics and in 2009 the lateral-directional case was emphasized. The test model used was the NASA Generic Transport Model (GTM) that represents a conventional twin-engine aircraft similar to that used in Ref. 4. A part of the 2007 data was used in Ref. 7 for modeling of longitudinal aerodynamics. For that study the steady data were obtained for different configurations and an extensive range of angles of attack. The dynamic tests included one degree-of-freedom forced oscillations around the pitch axis at different angles of attack, amplitudes, and frequencies. The postulated model in Ref. 5 and 6 was modified by defining the unsteady effect as a first-order dynamic system. A method of harmonic analysis was applied to measured longitudinal aerdynamic coefficients to allow estimation of the in-phase and out-of-phase coefficients. For estimation of parameters in the model an output error method was used that combined input and output time histories for each frequency into a single vector for time domain analysis.

In this paper the problem of system identification of a transport aircraft is considered again. This time, however, the oscillatory data in roll and yaw are analyzed using harmonic analysis and two other estimation techniques: a

nonlinear regression approach in the frequency domain and an output error method in the time domain. Although both methods are used to estimate unsteady parameters, damping, and cross derivatives at different angles of attack and amplitudes, for this paper, examples mainly demonstrate yawing moment coefficient models using a nonlinear regression method and a frequency domain model structure. This method is offered as an efficient method to determine dynamic derivatives and leads to a proposal for a single model for the yawing moment coefficient in the unsteady region. A limited example is provided to demonstrate the output error method and time domain model structure. As in previous model identification work, the resulting model is checked for prediction capabilities and sensitivity to parameter changes.

II. Measured Data

In order to obtain a more extensive lateral-directional aerodynamic data base for mathematical model identification, wind tunnel tests were conducted in 2009 at the NASA Langley 14x22 Wind Tunnel. A 5.5% scale model representing a conventional twin-engine commercial transport was tested. A diagram of the model showing its basic geometry is given in Fig. 1. Data included both roll and yaw forced oscillation experiments over a wide range of frequencies and amplitudes to allow unsteady model identification. For the roll case, wind tunnel speed was 92 fps and measurements were made for roll oscillations at angles of attack from -5 to 75 degrees, five frequencies of 0.06, 0.12, 0.23, 0.46, and 0.92 Hz, and four amplitudes of 5, 10, 20, and 30 degrees. For the yaw case, wind tunnel speed was 70 fps and measurements were made for yaw oscillations at angles of attack from -5 to 50 degrees, five frequencies of 0.05, 0.09, 0.18, 0.35, and 0.70 Hz, and four amplitudes of 5, 10, 20, and 30 degrees. The slower wind tunnel speed for yaw oscillations was used to ensure load limits for the balance were not exceeded. The frequencies chosen define the same non-dimensional frequencies, k=[0.015 0.028 0.054 0.108 0.215], for both roll and yaw tests. During the test runs data were obtained from 7 oscillation cycles for low frequency data and up to 44 cycles for the remaining data. Data were sampled at 250 Hz with low pass 100 Hz analog filters. The resulting data were further filtered with a 4 Hz low pass digital filter to remove unwanted frequency content. The filter was run in both directions to ensure no phase error was added to the data.

III. Mathematical Model

The model equations for the lateral coefficients, C_Y, C_n, and C_l, represented by C_a, where *a = Y, n, or l*, were developed from a general form of the indicial model equations presented in Refs. 2-3. Each coefficient is considered in the form

$$C_a(t) = C_a(0) + \int_0^t C_{a\beta}(t-\tau)\dot{\beta}(\tau)d\tau + \frac{b}{2V}\int_0^t C_{ap}(t-\tau)\dot{p}(\tau)d\tau + \frac{b}{2V}\int_0^t C_{ar}(t-\tau)\dot{r}(\tau)d\tau \tag{1}$$

where $C_{a_\beta}(t)$, $C_{a_p}(t)$, and $C_{a_r}(t)$ are the indicial functions and $C_a(0)$ is the initial value of C_a. Subscript *a* is used to represent *Y, n,* or *l*. Two assumptions were adopted to simplify the model: (a) the effect of angular accelerations $\dot{p}$ and $\dot{r}$ on any coefficient can be neglected and (b) the indicial functions in Eq. (1) can be expressed as

$$C_{a_\beta}(t) = C_{a_\beta}(\infty) - F_{a_\beta}(t) \tag{2}$$

where $F_{a_\beta}(t)$ is the deficiency function and $C_{a_\beta}(\infty)$ is the rate of change C_a with β evaluated in steady flow conditions.

The simplified model, which takes into account changes with respect to steady state, has the form

$$C_a(t) = C_{a_\beta}(\infty)\beta(t) + \frac{b}{2V}C_{a_p}(\infty)p(t) + \frac{b}{2V}C_{a_r}(\infty)r(t) - \int_0^t F_{a\beta}(t-\tau)\dot{\beta}(\tau)d\tau \tag{3}$$

To obtain a model appropriate for identification and with a limited number of parameters, the deficiency function is assumed to be a simple exponential function[9]

$$F_{a_\beta} = ae^{-b_1 t} \tag{4}$$

Models appropriate for an aircraft undergoing one degree of freedom forced oscillation in roll or yaw can be obtained using Eqs. (3) and (4). Considering one degree of freedom rolling motion in the tunnel

$$C_a(t) = C_a[\phi(t), p(t)] \tag{5}$$

where roll angle is related to the sideslip angle by the equation

$$\beta(t) = \sin^{-1}(\sin\alpha \sin\phi(t)) \tag{6}$$

Combining Eqs. (3-6), the aerodynamic models can be formulated as

$$C_a(t) = C_{a_\beta}(\infty)\beta(t) + \frac{b}{2V} C_{a_p}(\infty)\, p(t) - a\int_0^t e^{-b_1(t-\tau)}\dot{\beta}(\tau)d\tau \tag{7}$$

By introducing

$$\eta(t) = \int_0^t e^{-b_1(t-\tau)}\dot{\beta}(\tau)d\tau \tag{8}$$

and applying the Leibnitz integral rule, the state space form of Eq. (7) can be written as

$$\dot{\eta}(t) = -b_1\eta(t) + \dot{\beta}(t) \tag{9}$$

$$C_a(t) = C_{a_\beta}(\infty)\beta(t) + \frac{b}{2V} C_{a_p}(\infty)\, p(t) - a\eta(t) \tag{10}$$

From Eq. (7), a steady response can be obtained[9] as

$$C_a(t) = \bar{C}_{a_\beta}\phi_A \sin(\omega t) + \bar{C}_{a_p}\phi_A k\cos(\omega t) \tag{11}$$

Where ϕ_A is the amplitude of roll oscillation, k is reduced frequency, and $\bar{C}_{a_\beta}$ and $\bar{C}_{a_p}$ are the in-phase and out-of-phase components, respectively. These components are related to the model parameters (aerodynamic derivatives) by the equations[9]

$$\bar{C}_{a_\beta} = C_{a_\beta}(\infty)\sin\alpha_0 - a\frac{\tau_1^2 k^2}{1+\tau_1^2 k^2} \tag{12}$$

$$\bar{C}_{a_p} = C_{a_p}(\infty) - a\frac{\tau_1}{1+\tau_1^2 k^2}\sin\alpha_0 \tag{13}$$

For one degree of freedom yaw oscillations in the tunnel

$$C_a(t) = C_a[\psi(t), r(t)] \tag{14}$$

where yaw and sideslip angles are related by the equation

$$\beta(t) = \sin^{-1}(-\cos\alpha \sin\psi(t)) \tag{15}$$

The state space equations can be written as

$$\dot{\eta}(t) = -b_1\eta(t) + \dot{\beta}(t) \tag{16}$$

$$C_a(t) = C_{a_\beta}(\infty)\beta(t) + \frac{b}{2V}C_{a_r}(\infty)r(t) - a\eta(t) \tag{17}$$

and the corresponding in-phase and out-of-phase components[9] are expressed as

$$\bar{C}_{a_\beta} = C_{a_\beta}(\infty)\cos\alpha_0 - a\frac{\tau_1^2k^2}{1+\tau_1^2k^2} \tag{18}$$

$$\bar{C}_{a_r} = C_{a_r}(\infty) + a\frac{\tau_1}{1+\tau_1^2k^2}\cos\alpha_0 \tag{19}$$

IV. Model Identification

Measured oscillatory data in roll and yaw have been obtained at different angles of attack, amplitudes and frequencies. From carefully designed experiments these data provide information for determining adequate models for the lateral aerodynamics. These models have a postulated structure with parameters that can be estimated using the methods discussed in this paper. The last step in model identification is model validation where the models are evaluated as predictors.

A. Harmonic Analysis

A method of harmonic analysis[10] was applied to measured aerodynamic coefficients. A mathematical model for these coefficients is

$$C_a(t) = A_0 + \sum_{j=1}^{m} A_j \cos(j\omega t) + \sum_{j=1}^{m} B_j \sin(j\omega t) \qquad a = l, n \text{ or Y} \tag{20}$$

where A_0, A_j, and B_j are the Fourier coefficients. The analysis provides estimates of these coefficients, their standard errors, and the coefficient of determination, R^2. For the model with linear aerodynamics and A_0 = 0, the aerodynamic in-phase and out-of-phase components can be expressed in terms of the coefficients A_1 and B_1. For the roll oscillation case the expressions are

$$\bar{C}_{a_\beta} = \frac{B_1}{\phi_A} \tag{21}$$

$$\bar{C}_{a_p} = \frac{A_1}{k\phi_A} \tag{22}$$

and for the yaw oscillation case the expressions are

$$\bar{C}_{a_\beta} = \frac{B_1}{\psi_A} \tag{23}$$

$$\bar{C}_{a_r} = \frac{A_1}{k\psi_A} \tag{24}$$

where β is related to ϕ and ψ by Eqs. (6) and (15).

The coefficient of determination, R^2, indicates the fraction of the variation in the measured data explained by the model and is defined as

$$R^2 = 1 - SS_E / \mathrm{SS}_r \qquad 0 < R^2 < 1 \tag{25}$$

where

$$SS_E = \sum_{i=1}^{N} [C_{a_E}(i) - \hat{C}_a(i)]^2 \tag{26}$$

is the residual sum of squares and

$$SS_r = \sum_{i=1}^{N} [C_{a_E}(i) - \tilde{C}_a(i)]^2 \tag{27}$$

is the total sum of squares. $C_{a_E}(i), \hat{C}_a(i)$, and $\tilde{C}_a(i)$ are the measured, estimated, and mean values, respectively.

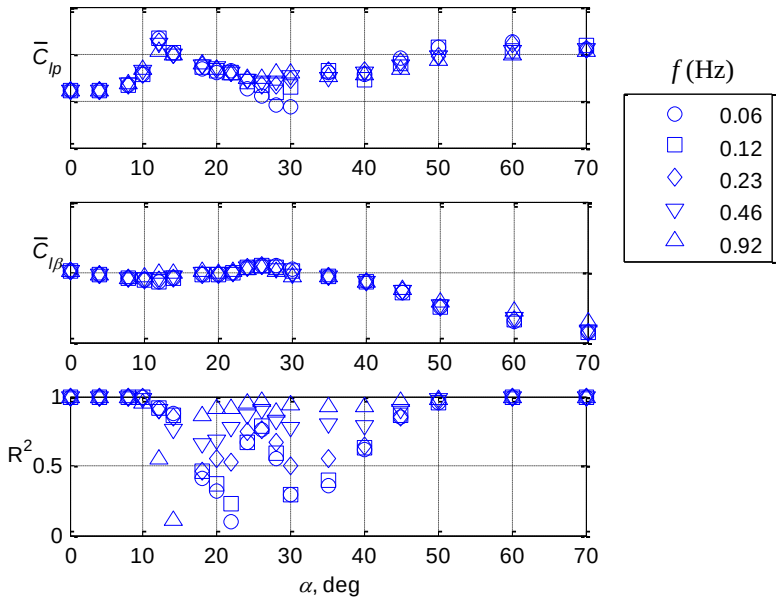

Figure 2. Harmonic analysis for rolling-moment coefficient, roll oscillations, ϕ_A=20°.

Harmonic analysis was performed on roll and yaw oscillatory data with amplitudes of 5º, 10º, 20º, and 30º. Example results of the analysis are presented in Figs. 2 and 3 for amplitudes ϕ_A = 20º and ψ_A = 20º, respectively. These plots show both in-phase and out-of-phase components and the coefficient of determination against angle of attack at different frequencies. Ordinate values were removed in order to maintain proprietary agreements. In both sets of results, the in-phase components show no dependence with frequency and therefore no unsteady aerodynamic effect. For the out-of-phase components, frequency dependence occurs for angles of attack between 24º to 30º for C_{l_p} and between 20º to 30º for C_{n_r}. For higher angles of attack the unsteady effect is very small and not significant for both coefficients.

Figures 2 and 3 reveal very large variation in R^2 for angle of attack above 20° for C_n and mostly above 18° for C_l. As follows from Eqs. (25) to (27), the estimates of R^2 are influenced by the value and number of Fourier coefficients (harmonic order) in Eq. (20) and the measurement noise in $C_{a_E}(i)$. Because the Fourier coefficients are mutually orthogonal, the estimates of A_j and B_j will not change with the number of coefficients included in Eq. (20). Changes will only appear in the corresponding standard errors and residuals defined by Eq. (26). This makes R^2 an effective diagnostic tool to discern the adequacy of a linear first-order model against nonlinear higher harmonic models.

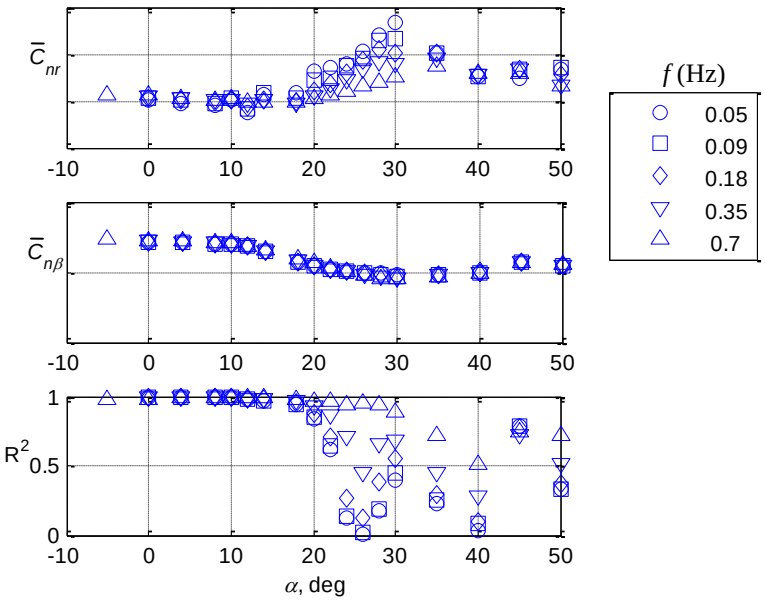

Figure 3. Harmonic analysis for yawing-moment coefficient, yaw oscillations, ψ_A=20°.

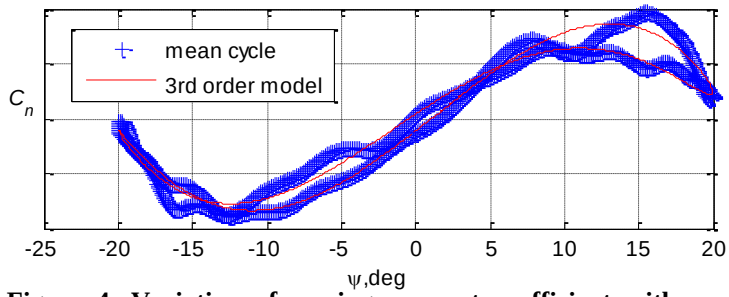

Figure 4. Variation of yawing moment coefficient with yaw angle is shown for one cycle of 3rd order harmonic model and the mean cycle of measured data (α_0=30º, ψ_A=20°, f= 0.18Hz).

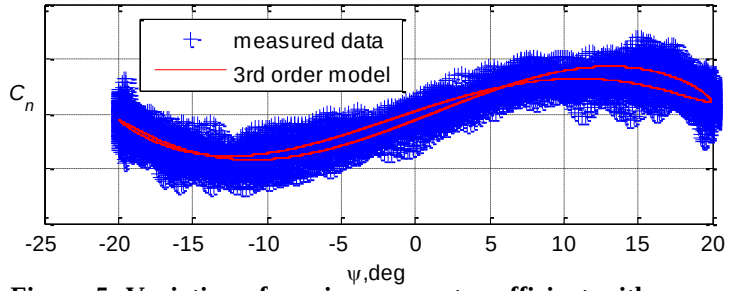

Figure 5. Variation of yawing moment coefficient with yaw angle is shown for one cycle of 3rd order harmonic model and all cycles of measured data (α_0=30º, ψ_A=20°, f= 0.18Hz).

Figure 4 shows measured $C_n(\psi)$ time histories, in phase plane format, for one oscillation cycle at α_0 = 30º, f = 0.18 Hz, and ψ_A = 20 degrees. The single oscillation cycle shown with "+" signs is the mean cycle of all the measured data. An estimated 3rd order harmonic model is shown as a solid line. The cubic model fits the measured data well and an R^2 = 0.81 suggests this is an adequate model. A first order model produces R^2 = 0.55 and implies that a higher order model is required in this case. When using R^2 to assess model order adequacy measurement noise is a confounding factor. Consequently, the R^2 threshold for an adequate model can be lower as the severity of measurement noise increases. The noise and repeatability of each oscillation measurement is demonstrated in Fig. 5, showing the same case as Fig. 4 but with all oscillation cycles included. The average measurement standard error is approximately 0.004 at each point in the cycle. This is a relatively large number for measurements with an approximate maximum range of ± 0.01 from the mean at each point in the cycle. Extending this analysis over the full range of nominal angles of attack, α_0 , at the same amplitude and frequency (f = 0.18 Hz, ψ_A = 20 degrees), Fig. 6 shows variation of R^2 with the number of harmonics. Poor model adequacy is indicated for 1st and 2nd order models for α_0 > 22º, however, acceptable model adequacy is achieved with 3rd order models. Low R^2 values for the cubic models, for example at α_0 = 24º or 40º, are due to high measurement noise levels and poor signal-to-noise ratio. At α_0 = 40º the average measurement standard error is approximately 0.008 at each point in the cycle. This is twice the noise level found at α_0 = 30º. Fig. 7 shows variation of R^2 with amplitude and frequency for the nominal angle of attack at α_0 = 30º and for 1st order harmonic models only. As expected, larger amplitude oscillations produce more nonlinear responses and therefore lower values of R^2. Less obvious is the strong correlation of lower R^2 values with lower frequency. This relationship is explained using nonlinear models in the next section under *Output Error* analysis. From the harmonic analysis, as shown in Figs. 2 to 7, aerodynamic model structures for C_n and C_l can be characterized in the following way:

a.) Conventional linear models without an unsteady component are adequate for yawing moment models where $\alpha_0 < 20^o$. Similarly, a conventional linear model structure without an unsteady component applies to rolling moment models where $\alpha_0 \leq 10^o$. Outside of these regions one of the three model components in Eqs. 10 and 17 (steady aerodynamics, steady-flow damping, unsteady aerodynamics) may require a nonlinear model structure.

b.) The strongest presence of unsteady aerodynamics are found in the yawing moment response for $20^o \leq \alpha_0 \leq 30^o$ and in rolling moment response for $24^o \leq \alpha_0 \leq 30^o$.

c.) Final assessement of each model component is made in the next section under *Output Error* analysis where relative magnitudes of the model terms are compared.

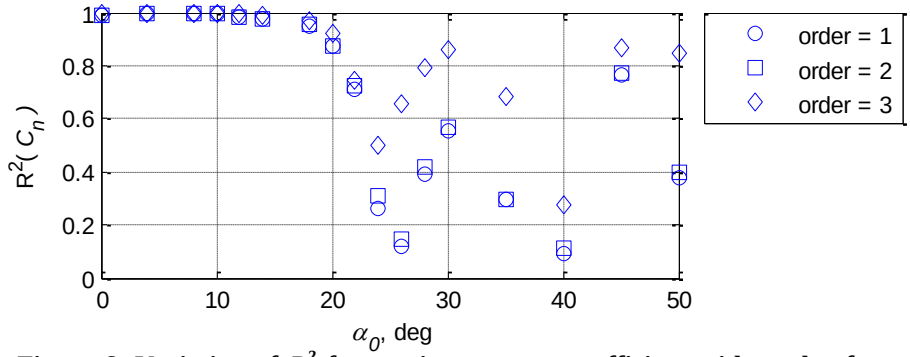

Figure 6. Variation of R^2 for yawing moment coefficient with angle of attack and number of harmonics, (ψ_A=20°, f= 0.18Hz).

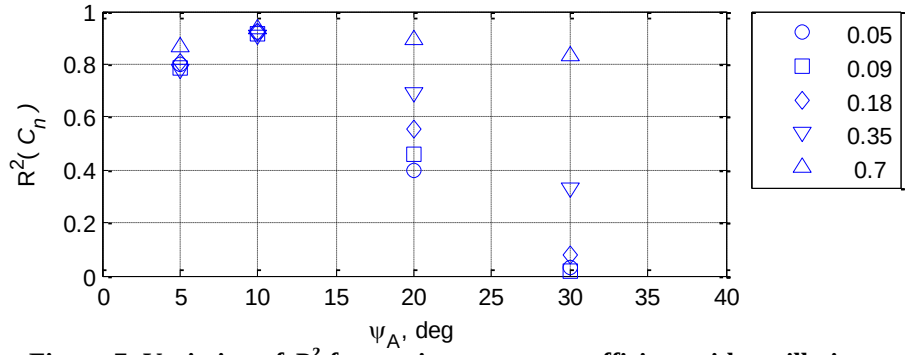

Figure 7. Variation of R^2 for yawing moment coefficient with oscillation amplitude and frequency, (α_0= 30°, harmonic order = 1).

B. Parameter Estimation

Parameter estimation was accomplished using two techniques: a nonlinear regression (NR) method in the frequency domain, and an output error (OE) method in the time domain. Both techniques are explained in Ref. 11 where the relevant computer programs are available. For the NR analysis only the out-of-phase component data were used in conjunction with Eq. (13) for roll motion and Eq. (19) for yaw motion. In-phase components were not used in the calculations because of the significant lack of frequency dependence. For the OE approach the model equations are given by Eqs. (9-10) for roll motion and Eqs. (16-17) for yaw motions. Measured inputs, $\dot{\beta}$, and outputs, C_a, for each of the five frequencies tested, were stacked to ensure all the frequency content was included in the time domain estimation process.

As a practical matter to limit discussion in this paper, estimation results are presented with a focus on developing linear unsteady models for yawing moment using the NR method. The final model proposed is offered to represent the unsteady aerodynamic behaviors for the yawing moment over the region of angle of attack, $20^o \leq \alpha_0 \leq 30^o$, with unsteady aerodynamic response.

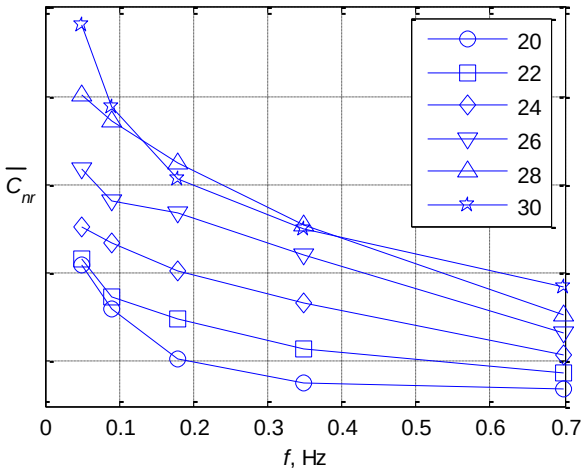

Figure 8. Variation of out-of-phase components with frequency and angle of attack. Yaw oscillatory data, ψ_A=20°.

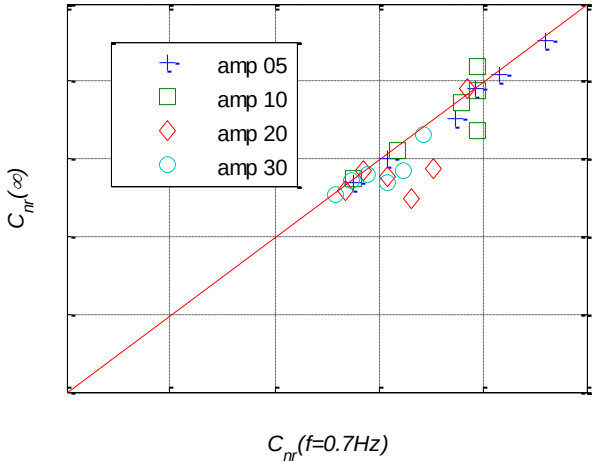

Figure 9. Estimated damping parameters from yaw oscillatory data, unsteady region (20°<α_0<30°), using harmonic analysis and nonlinear regression.

1. Nonlinear Regression

To demonstrate the NR technique, results addressing the damping-in-yaw case are presented. Model structure is defined by Eq. (19) and for this case takes the form

$$\bar{C}_{n_r}(j) = C_{n_r}(\infty) + a\frac{\tau_1}{1+\tau_1^2 k^2(j)}\cos\alpha_0 + \nu(j) \qquad j = 1,2,...,m \tag{28}$$

In this formulation $\bar{C}_{n_r}$ is the measured dependent variable, k is the regressor, a, τ, and $C_{n_r}(\infty)$ are the unknown parameters, and ν is the measurement noise. A potentially useful observation can be taken from Eq. (28) by considering the limiting case for $k \to \infty$. In this case as k becomes large, the out-of-phase component, $\bar{C}_{n_r}$, approaches $C_{n_r}(\infty)$ in value. This suggests a unique method for an experimenter to estimate $C_{n_r}(\infty)$ by just testing at sufficiently high frequency. Figure 8 provides evidence that a limiting value is approached for higher frequencies. Shown in Fig. 8 are the variations of out-of-phase components, $\bar{C}_{n_r}$, with frequency and angle of attack for large amplitude ($\psi_A = 20°$) yaw oscillatory data. Figure 9 demonstrates the limiting relationship, $\bar{C}_{n_r} \approx C_{n_r}(\infty)$, is a reasonable assumption for the cases considered. Shown are estimated damping parameters using yaw oscillatory data in the unsteady region (20° < α_0 < 30°) with four different amplitudes. The solid diagonal line shows the exact values for which ordinate and abscissa values are equal.

Parameter estimates and their 2-σ error bounds for the model in Eq. (28) are shown in Fig. 10. The results show low standard errors for parameters $C_{n_r}(\infty)$, a, and τ over the range of angle of attack with unsteady responses. At α_0 = 26° some larger error bounds occur in $C_{n_r}(\infty)$ and a. This corresponds to the lower R^2 values from harmonic analysis which infer the likelihood of nonlinear behaviors. $C_{n_r}(\infty)$ is relatively constant over this range of α_0, however parameter a trends toward zero for α_0 < 20°, reflecting the lack of unsteady behavior in that flight regime. Poor parameter accuracy for nondimensional τ at α_0 < 20° also reflects the lack of unsteady behavior.

2. Output Error

Both estimation methods (NR and OE) used in this study are nonlinear estimation methods and both have been applied to estimate parameters associated with linear aerodynamic model structures. Both methods can also be applied to estimate all damping and cross derivatives terms. However, when nonlinear model structures are required the OE method must be applied. To demonstrate the OE method, only one example is considered where the static term is replaced by a cubic polynomial. Reference 12 provides a full description of the more general nonlinear case using OE.

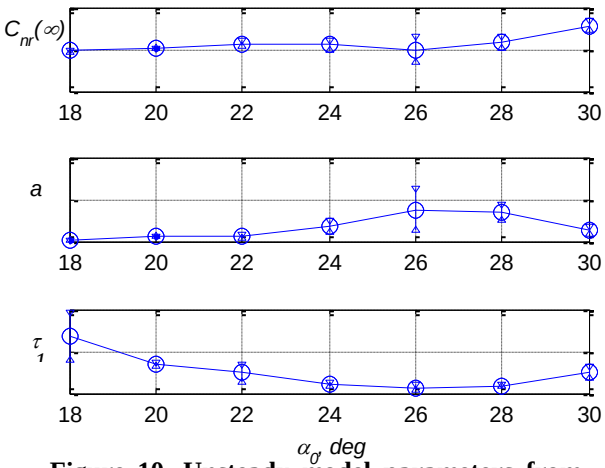

Figure 10. Unsteady model parameters from NR method for yaw oscillatory data, ψ_A=20º.

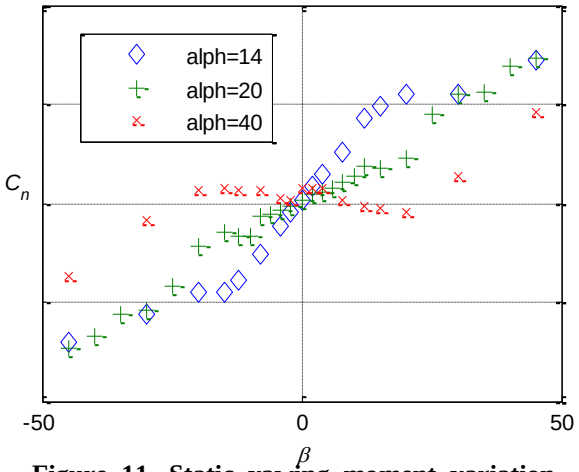

Figure 11. Static yawing moment variation with sideslip for α_0 = [14º, 20º, 40º].

The linear model structure is defined by Eqs. (16-17) and for this case the state space equations can be written as

$$\dot{\eta}(t) = -b_1\eta(t) + \dot{\beta}(t) \tag{29}$$

$$C_n(i) = C_{n_\beta}(\infty)\beta(i) + \frac{b}{2V}C_{n_r}(\infty)r(i) - a\eta(i) + \upsilon(i) \qquad i = 1,2,...,N \tag{30}$$

Replacing the static term by a cubic polynomial in β is suggested by the harmonic analysis results that showed improved R^2 for a 3rd order harmonic model. For this case, an adequate model was achieved by allowing a cubic polynomial model structure for the static term while retaining a linear structure for the two dynamic terms.

The OE method requires an initial guess of the four unknown parameters ($C_{n_\beta}(\infty)$, $C_{n_r}(\infty)$, a, b_1) in Eqs. (29-30) to start the optimization process. If a four term cubic polynomial is used for the static term then the number of unknowns is seven. When static data or NR estimates are available these values can be used directly as initial values otherwise engineering estimates are required to provide starting values. To simplify obtaining the intial parameter values and the general estimation process, starting with linear model first works well. For the more general model, a three-stage estimation process is used. In the first stage only static terms are estimated. In the second stage the static terms are fixed and only dynamic terms are estimated. In the final stage, all the terms are estimated using the estimates from stage one and two as the starting values.

For the yawing moment the underlying static curve, $C_n(\infty;\alpha_0,\beta)$, changes significantly when moving from low to high angles of attack. Figure 11 shows these static curves for three different α_0 = [14º, 20º, 40º]. For the lower α_0 the change in $C_n(\infty;\alpha_0,\beta)$ is linear over a relatively wide range of β, however, for $\alpha_0 \geq$ 20º a significant cubic nonlinearity develops near β = 0 and $C_{n_\beta}(\alpha_0)$ changes slope from positive to negative. Incorporating a cubic static term into the model structure of Eq. (30) while maintaining the linear terms for both steady flow damping and unsteady terms allowed estimation of improved models. An example of the improved model fit to the data is shown in Fig. 12 for the case where $\psi_A = 20°$ and α_0 = 26º. This case was chosen due to the very low values of R^2 obtained during harmonic analysis, where the low values at low frequency (see Fig. 3) implied that linear model adequacy was very poor. Using the OE method for the same case and forcing a linear model structure for all terms produced R^2 = 0.34 and a poor fit between measurements and computed responses, especially at lower frequencies. After allowing a cubic static nonlinearity in the model structure the fit improved so that R^2 increased to 0.58, an acceptable value given the relatively poor signal/noise conditions for this case. The severity of the noise can be observed in the low frequency case (upper left hand graphic) of Fig. 12 where the respone for lower frequencies approach a quasi-static response and more closely follow the underlying static curve. The dominating effect of the damping terms can be seen in the high frequency case (lower right graphic) where the effects of the underlying cubic static curve are almost removed. The dominating effect of the steady damping term over the static term at high frequency also

explains the observation made in the harmonic analysis section that reduced R^2 values (less linear response) occur with lower frequencies.

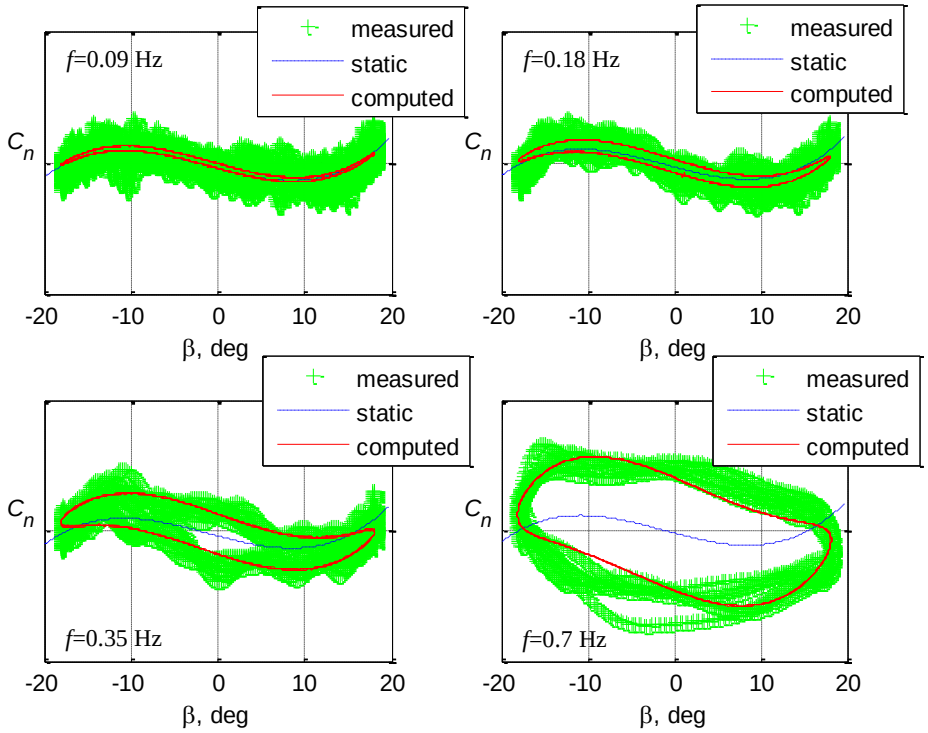

Figure 12. Variation of C_n under forced oscillation in yaw. Six cycles of measured and OE model responses are shown for at α_0 = 26°, ψ_A=20°, f= 0.09, 0.18, 0.35, and 0.70Hz.

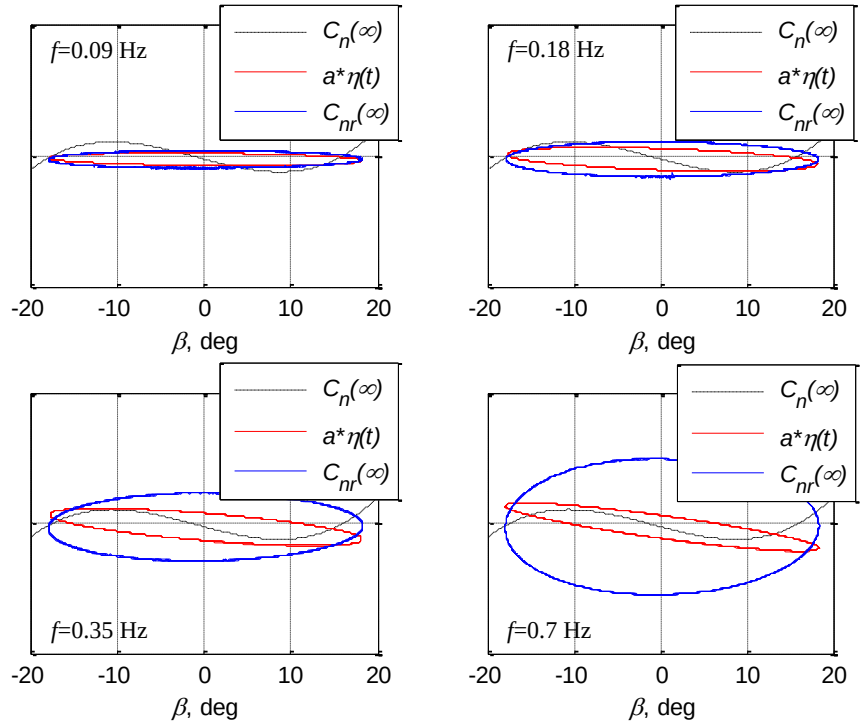

Figure 13. C_n component responses from OE model are shown for α_0 = 26°, ψ_A=20°, f= 0.09, 0.18, 0.35, and 0.70Hz.

A key aspect of this system identification problem is determining the appropriate model structure. In an effort to obtain a parsimonious model it is useful to approach the system identification problem using linear model structures to determine their efficacy first so model complexity is only applied where necessary. The analysis so far has produced appropriate models that can be readily used for simulation and control design. However, engineering judgment is required to assess the utility of the added complexity. This may require piloted simulation to determine the ultimate efficacy of a linear or nonlinear unsteady model. However, a quick evaluation of the model can be done by considering each terms' relative contribution to the total force or moment. Shown in Fig. 13 are the three components of Eq. (30) for the yawing moment using the same model parameters as used for Fig. 12. Specifically, the cubic static term, $C_n(\infty,\beta)$, steady flow damping, $C_{n_r}(\infty)$, and unsteady component, $a*\eta(t)$, are each plotted separately to show their relative contribution to the total response seen in Fig. 12. In Fig. 13, one can observe for this aircraft configuration, that for the lower frequencies the static terms will dominate the response and at high frequencies the steady flow damping term will dominate. In the mid-frequencies the

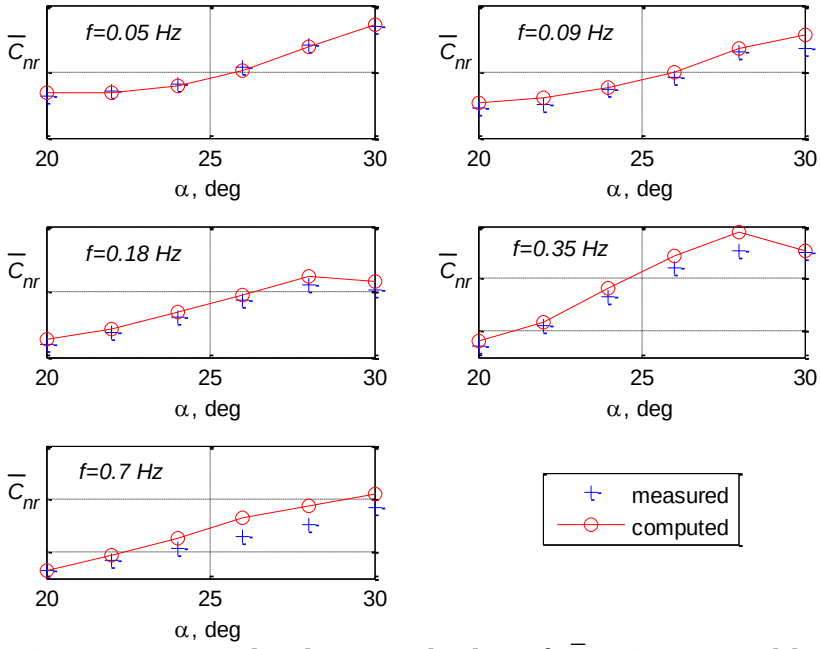

Figure 14. Measured and computed values of $\bar{C}_{n_r}$ using NR model for yaw oscillatory data, α_0 = 28º, ψ_A=20°.

unsteady component makes a contribution comparable to the steady flow damping term. These results indicate an approach that can be used to estimate higher fidelity models with nonlinear components if required. Engineering judgment is required to determine if the added complexity is needed.

C. Model Validation

In this study, the focus was to introduce a nonlinear regression method and frequency domain model to allow estimation of linear unsteady aerodynamic models for aircraft. Satisfaction of an adequate model is achieved by demonstrating good fit to the measured data used in estimation and an ability to predict on other data. Figure 14 shows out-of-phase component measurements, $\bar{C}_{n_r}$, and computed values determined from the estimated model. The comparison shows a tendency to a better fit at the lower frequencies, however, differences at higher frequencies shown in Fig. 14 did not produce a large error in the total yawing moment. Because of the relatively smaller contribution of the unsteady component in general and in particular at higher frequencies, it seems reasonable to postulate using an "average" unsteady model over the entire unsteady region. The "average" unsteady model was created by taking the average of each NR model parameter estimate over the six α_0 cases

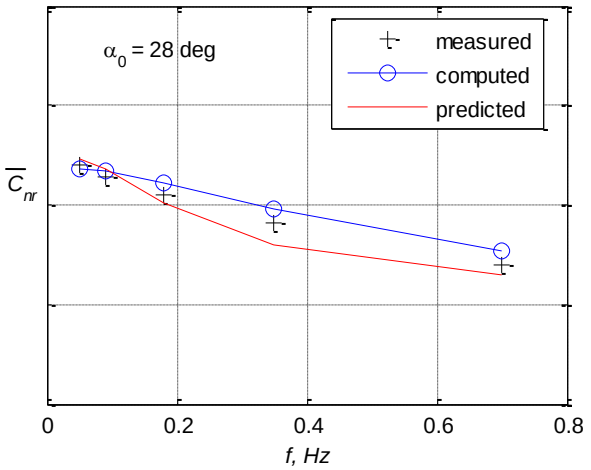

Figure 15. Measured, computed, and predicted values of $\bar{C}_{n_r}$ for yaw oscillatory data, α_0 = 28º, ψ_A=20°.

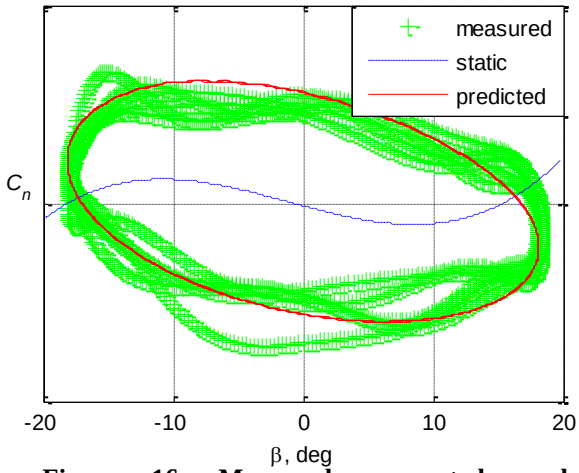

Figure 16. Measured, computed, and predicted values of $C_n(t)$ for yaw oscillatory data, α_0 = 28º, ψ_A=20°, f = 0.7 Hz.

considered in the angle of attack range, 20º ≤ α_0 ≤ 30º. The linear model static term for the "average" model was taken from an average of the OE linear model estimates. As an example, in Fig. 15 model performance is evaluated by comparison of the "average" model prediction of $\bar{C}_{n_r}$ values plotted with estimated or "computed" model values and measured values at each frequency, for α_0 = 28º. An additional check of this new "average" model's predictive

capability is shown in Fig. 16 where a phase-plane plot for the same α_0 = 28º case, and f = 0.7 Hz, is shown. In this figure measure data for several oscillations are shown with the "average" model prediction shown as the solid line. The dashed static line, showing a cubic polynomial shape, is provided for reference. However, the cubic static term was not used in the "average" model. The graphic shows a reasonable prediction of the response by the "average" linear model.

V. Concluding Remarks

This paper expands on previous model identification work using the NASA Generic Transport Model. The emphasis for this paper was on modeling methodology rather than an extended presentation of specific modeling results. Tests in the NASA LaRC 14x22 wind tunnel provided forced oscillation data in roll and yaw over extended range of angle of attack, frequency, and amplitude.

A method of harmonic analysis, used as an analysis and diagnostic tool, revealed the dependence of conventional damping terms (in-phase and out-of-phase components) and coefficient of determination on angle of attack, frequency, and amplitude of oscillation. Behavior of the coefficient of determination was discussed and used to aid in selection of a parsimonious model structure.

Mathematical model formulations were proposed for one-degree-of freedom rolling and yawing motion with linear unsteady aerodynamics. Two approaches were presented and application was demonstrated using the yawing motion coefficient. One approach used nonlinear regression and a frequency domain model structure. This approach was proposed as a simple and efficient method to model the unsteady aerodynamic behavior for this aircraft. Because estimates of the in-phase component showed no significant variation with frequency, only out-of phase components were used. Linear unsteady models were identified and presented for the yawing moment coefficient over the range of alpha where unsteady behaviors occurred. Each model included estimates of a damping derivative and two parameters of the deficiency function. A single model for the entire unsteady region was also suggested as a potential candidate. Using the model formulation for the nonlinear regression method, it was shown that with increasing frequency the out-of-phase components approach the steady values of the corresponding damping derivatives.

A second approach presented used an output error estimation method and a time domain model structure in state-space format. This approach includes parameters for both static and dynamic parameters and can accommodate nonlinear behaviors. An example was presented for a case where static nonlinear behavior was found in the aerodynamic coefficient with respect to sideslip. An approach is suggested for evaluating the necessity of this added complexity.

Application of this modeling methodology will allow identification of unsteady models from static and dynamic wind tunnel data. These models will support advanced simulations of transport aircraft throughout the flight envelope and in turn facilitate advanced aircraft control designs that provide stability and control in difficult flight regimes.

Acknowledgments

The authors would like to thank Mr. Gautam Shah from NASA Langley Research Center for providing the experimental data and for numerous discussions on data handling.

References

[1]Jones, Robert T. and Fehlner, Leo F., "Transient Effects of the Wing Wake on the Horizontal Tail," NACA TN-771, 1940.

[2]Tobak, Murray, "On the Use of Indicial Function Concept in the Analysis of Unsteady Motions of Wings and Wing-Tail Combinations, NACA Rep. 1188, 1954.

[3]Klein, Vladislav, "Modeling of Longitudinal Unsteady Aerodynamics of a Wing-Tail Combination," NASA CR-1999-209547, September, 1999.

[4]Khrabrov, A., Vinogradov, Yu, and Abromov, N., "Mathematical Modeling of Aircraft Unsteady Aerodynamics at High Incidence with Account of Wing-Tail Interaction," AIAA Atmospheric Flight Mechanics Conference, AIAA 2004-5278, AIAA Washington, DC, 2004.

[5]Murphy, Patrick C. and Klein, Vladislav, "Estimation of Longitudinal Unsteady Aerodynamics of a Wing-Tail Combination from Wind Tunnel Data," AIAA Atmospheric Flight Mechanics Conference, AIAA 2006-6154, AIAA Washington, DC, 2006.

[6]Murphy, Patrick C. and Klein, Vladislav, "On Problems Associated with Modeling Wing-Tail Configurations from Wind Tunnel Data," AIAA Atmospheric Flight Mechanics Conference, AIAA 2007-6722, AIAA Washington, DC, 2007.

[7]Shah, Gautam H., et. al, "Wind-tunnel Investigation of Commercial Transport Aircraft Aerodynamics at Extreme Flight Conditions," SAE Technical Paper 2002-01-2912, 2002.

[8]Brandon, Jay M., et. al, "Comparison of Rolling Moment Characteristics During Roll Oscillations for a Low and High Aspect Ratio Configuration," AIAA Atmospheric Flight Mechanics Conference, AIAA 2004-5273, AIAA Washington, DC, 2004.

[9]Klein, Vladislav and Norderer, Keith D., "Modeling of Aircraft Unsteady Aerodynamic Characteristics. Part I – Postulated Models," NASA TM 109120, May, 1994.

[10]Klein, Vladislav, Murphy, Patrick C., and Szyba, Nathan M., "Analysis of Wind Tunnel Oscillatory Data of the F-16XL Aircraft," NASA TM-2004-213246, August, 2004.

[11]Klein, Vladislav and Morelli, Eugene, "Aircraft System Identification: Theory and Practice," 1st edition, AIAA Inc., Reston, Virginia, 2006.

[12]Murphy, Patrick C., Klein, Vladislav, and Szyba, Nathan M., "Progressive Aerodynamic Model Identification From Dynamic Water Tunnel Test of the F-16XL Aircraft," AIAA Atmospheric Flight Mechanics Conference, AIAA 2004-5277, AIAA Washington, DC, 2004.